Numerical simulation of cellular tip growth

Bruno Denet
Institut de Recherche sur les Phénomènes Hors d'Equilibre, Groupe de Biophysique, Université de Provence–Centre de Saint Jérôme, UMR 138 (S 252), 13397 Marseille Cedex 20, France
(Received 30 January 1995)

Numerical simulations of a model for cellular tip growth are performed, using a Green's function formalism. In this model, cellular growth is coupled to a morphogen concentration outside the cell. Typical shapes are obtained, and compare satisfactorily to experimental results.

PACS number(s): 87.22.As, 87.22.Fy

I. INTRODUCTION

Growth at the unicellular level can occur in two basic manners [1]: diffuse growth and tip growth. The first mechanism corresponds essentially to uniform expansion of the cell wall, while in the second expansion is limited to a particular zone of the membrane. As a result of this kind of cellular growth, cells often become cylindrical, that is, a rhizoid shape, expansion being confined to an apical dome at the end of the cell. A variety of different cells grow in this manner; for example, root hairs, hyphal cells observed in fungi, and pollen tubes [2]. Another well-known example is the neuron. In this case, the neural axon exhibits the cylindrical shape previously described. Each dendrite tip is also growing because of the same type of phenomenon and takes the form of a growth cone, although in this last case there is also continuous secondary branching. Related effects are also observed in unicellular algae, for instance, *Micrasterias rotata* [3]. In this case, several lobes are formed in the cell wall, and during the growth each lobe enlarges: this is called lobe broadening. When the lobe is sufficiently large, it breaks in two and this is called lobe branching.

All these observations closely resemble other propagating front experiments, such as solidification fronts, Saffman-Taylor fingers, or flames (see, for instance, [4] for a review). There is thus the hope to use this analogy in order to obtain theoretical models of tip growth, taking into account, of course, the specificities of biological phenomena. A first step in this direction has been the use of geometrical models of morphogenesis [5]. These models are similar to the geometrical model in dendrite growth [6], and describe normal growth velocity at a given point of the front only in terms of local quantities such as the curvature and its derivatives. Shapes similar to the experimental results have been obtained by numerical simulations of this model [7].

However, as in the solidification case, it is now necessary to obtain more realistic and nonlocal descriptions of the growth. The model of Hentschel and Fine [8] is promising: the normal velocity at a point of the interface is considered to be a function of a morphogen concentration which satisfies a diffusion equation, the concentration flux at the interface being also concentration dependent.

In this paper, we will solve numerically a modified version of the Hentschel-Fine model, in which the morphogen is located outside the cell. The model will be described in Sec. II. We will suppose that the concentration field can be supposed quasistationary in the reference frame moving with the tip, and the equations will be described in this approximation in terms of Green's functions in Sec. III, with also a description of the numerical method used in the simulation. The results concerning the possible shapes of the tip will be described in Sec. IV.

II. MODEL

The original Hentschel-Fine equations [8] correspond to a morphogen located inside the cell, which satisfies a diffusion equation and whose flux at the membrane is a function of the local concentration. The normal velocity at the current point on the interface is also assumed to be a function of the local concentration. In some papers, it has been attempted to describe the growth only in terms of elongation of the cell surface and not in terms of normal velocity; see, for instance, [9], where a model of algal growth considering the coupling between an interface and a reaction diffusion prepattern was considered. However, it has been emphasized in [5] that the elongation rate does not determine cell growth in a unique way, contrary to normal velocity, and that there is a relation between elongation rate and normal velocity that depends on the tangential velocity of the particles incorporated in the membrane. So in the geometrical models of [5] and [7], two laws were assumed, one on the elongation rate, and the other on the tangential velocity. On the contrary, in [8], there is only one law on the normal velocity, and it has the same effect of completely describing cellular surface growth.

In this paper, the authors have in mind the growth of dendritic arbors in neurons and the calcium ion as a morphogen, which can act as a catalyst of polymerization (and depolymerization) reactions involved in cytoskeletal formation. The essential reactions of this type concern tubulin and actin, and depend on the value of the inner concentration of calcium. Assuming that the normal velocity depends in a bell shaped manner on the submembrane calcium concentration, a stability analysis of the circular shape has been performed and it has been shown that two types of instabilities are possible: a spontaneous

ionic current instability at constant shape can occur; then leading to a shape modification of the ionic current is carried by a morphogen. There is also the second possibility of a coupled instability of both the form and the ionic current pattern.

The calcium flux at the membrane is carried by voltage dependent calcium specific ion channels, and can be an important part of the total ionic currents observed in some systems [10], such as the zygotes of the brown algae *Fucus* or *Pelvetia* during tip growth [11]. These algae have been a common system for morphogenesis studies. However, the calcium ion channels have the very specific property that the calcium influx increases when the membrane depolarizes, and this voltage dependence could be sufficient to create a spontaneous instability of the ionic current pattern at constant shape (see [12] and [13] for a theoretical and a numerical study of this effect). Another possible explanation of the ionic current pattern observed in the *Fucus* zygote prior to any growth is based on the mobility of calcium channels and pumps on the membrane [14].

On the other hand, diffusive morphogens different from the calcium ion exist, for instance in the case of growth of hyphae in fungi, amino acids such as methionine in the water mold *Achlya bisexualis* [15], or acetylcholine in the neuron case. However, these morphogens are often located outside the cell, and their concentration can control the growth. These morphogens are called chemoattractants because a modification of their concentration can curve the tip (this is called chemotropism) or induce side branching [16,17]. The flux of these chemoattractants is associated with the ionic current pattern: for instance, the amino acids are carried by a symport together with the H^+ ion. So we consider a model where the morphogen is located out of the cell; let us denote its concentration by C and its concentration at infinity by C_∞. We will use in the following the normalized concentration

$$u=(C-C_\infty)/C_\infty$$

which varies from 0 at infinity to -1 if there is no morphogen concentration at all (we have found in the simulations that u is always negative): it satisfies a diffusion equation with diffusion coefficient D:

$$\frac{\partial u}{\partial t}=D\Delta u \ . \tag{1}$$

In all the simulations, we have kept the diffusion coefficient equal to 1. Furthermore, as in the Hentschel-Fine model, the normal influx at the membrane is given as a function of the local concentration:

$$D\frac{\partial u}{\partial n}=j(u) \ . \tag{2}$$

The local normal velocity of the interface is also a function of the local morphogen concentration:

$$v_n=v(u) \ . \tag{3}$$

This model contains two unknown functions $j(u)$ and $v(u)$, but it should be possible to measure these functions experimentally. We have now to specify the two functions we will use in the following. We will take the simplest possible form for $j(u)$, namely, a linear dependence on u,

$$j(u)=u-u_0 \ , \tag{4}$$

where u_0 will take the constant value -0.15 in all the simulations. The flux $j(u)$ has here a positive slope versus the normalized concentration u: the higher the outer concentration, the higher the morphogen flux entering the cell. This positive slope corresponds to the most common situation; let us note, however, that in the case of calcium the slope can be negative for sufficiently high external calcium concentrations [11].

Let us now discuss the interface normal velocity $v(u)$. First of all, contrary to the Hentschel-Fine model where the submembrane calcium concentration acts as a catalyst of chemical reactions related to cytoskeletal formation, here the relation between the outer morphogen concentration and the normal velocity is less direct. There is much experimental evidence of outer morphogens controlling tip growth, but we do not have in all cases a precise idea of the actual mechanism involved. It is likely that this mechanism depends on the important morphogen in a particular biological system. But anyway there will be coupling, for instance, through control of inside calcium concentration in the acetylcholine case, between the morphogen concentration and formation of actin filaments, microtubules, or other microfibrils inside the cytoplasm.

In the example previously quoted of the water mold *Achlya bisexualis,* the morphogen is an amino acid which is a nutrient for the cell, providing nitrogen, sulfur, and perhaps energy [18]. It is thus not very surprising that this type of morphogen has an effect on cell growth, but in this case the effect is local. The amino acid enters the cell by symport with the H^+ ion, and probably controls the concentration of apical vesicles which fuse with the apical membrane and provide new material necessary for cell wall formation. It is generally believed that the vesicles are produced far from the tip and have to travel toward the apex, for instance, by a vectorial transport mechanism, but this point has not been demonstrated, and it is possible that the vesicles are produced apically, in a coherent structure called *Spitzenkörper* [10].

So here, as in Hentschel and Fine's work, we make the simplifying assumption that the normal velocity is simply a function of the concentration. This is of course a phenomenological description of a phenomenon which depends on different factors: turgor pressure, cell wall synthesis, and cytoskeletal formation. However, as we do not have at this stage quantitative indications on these different effects, a global description of the growth at a macroscopic level is mandatory, which leads to the experimentally well-established notion of growth controlled by morphogen concentration.

Furthermore, we are only interested here in tip growth, and we have to choose the function $v(u)$ in order to obtain this type of effect. Of course, if the normal velocity was only slightly dependent on the concentration, then we would obtain a more or less uniform expansion of the

cell, and it would result in diffuse growth. In tip growth, on the contrary, we have different zones on the cell: the active zone where the growth phenomena are localized and a frozen zone where practically nothing happens. Often there is a change in the chemical structure of the membrane (and the cell wall in the case of plant cells) between these two regions (see [19] in the case of hyphal growth in fungi).

This form of the dependence of the normal velocity on concentration will be the one suggested by experiments. For instance, in experiments on side branching [16], for a low concentration of morphogen the normal velocity is exactly zero on the (plane) tip side: this corresponds to the frozen zone. If the concentration is increased locally above a certain threshold, then the local normal velocity increases with concentration; this is the active zone. The rigidity of the membrane has also to be taken into account, in order to prevent small-scale disturbances from becoming linearly unstable. We will take a function of the form

$$v(u)=\begin{cases} au+b+\gamma\dfrac{\partial^2\kappa}{\partial s^2} & \text{if } u>u^*=-b/a \\ \gamma\dfrac{\partial^2\kappa}{\partial s^2} & \text{if } u<u^*, \end{cases} \tag{5}$$

where κ is the curvature, s the curvilinear coordinate on the interface, and a, b, and γ are positive numbers. In Eq. (5), a is positive: the normal velocity increases with outer morphogen concentration in the active zone. The term in γ is of the form taken previously in [8] and [7]. In the terminology of [8], we will call in the following the coefficient γ the "effective rigidity," but one should remember that it is not the rigidity coefficient occurring in equilibrium elasticity. So, below the value u^*, we have a frozen zone where only "rigidity" effects are present.

We would like to emphasize that, although we have here expressed the normal velocity as a function of the rescaled variable u, it is actually a function of the physical concentration C. In this variable, the frozen zone corresponds to $C<C^*$. If we take a small value of $C_\infty(<C^*)$, the concentration C will be smaller everywhere in the domain, and thus smaller than C^*: the interface will be completely frozen. So with no morphogen or with only a small amount of morphogen there is no growth at all in this model. This effect can be observed in experiments [16]; however, in a lot of experimental cases there are several morphogens present in the extracellular medium, and not only one, as in the Hentschel-Fine type of models.

The problem now is to solve the previous set of equations, particularly the diffusion equation in a domain limited by a moving boundary. This is not a simple task, but we can observe the analogy of these equations with the one-sided model of crystal growth. In the next section, we will describe a Green's function formulation of this model valid in a quasistationary approximation.

III. GREEN'S FUNCTION FORMULATION

In this paper, we are not interested in the linear stability of any basic solution such as the circular one, but only in solutions where a well-defined tip will form and advance. The situation is then relatively similar to the advance of a solidification front in a supercooled melt, where the solution is close to an Ivantsov parabola. In this case, the normal front velocity is also coupled to diffusion fields that satisfy boundary conditions at the interface. Green's functions formulations, together with boundary element methods, have been used successfully to obtain numerical solutions of the dendritic shape in the solidification problem, in stationary [20] as well as nonstationary cases [21]. Of particular interest to us is the one-sided model of crystal growth, where the diffusion is assumed to take place only in the liquid, which is not very different from the model with a morphogen outside the growing cell that we have described in the previous section. We will perform here nonstationary numerical simulations of this morphogenesis model, and it will be relatively similar to the same type of simulations for the one-sided solidification model (see [21]).

Let us define x to be the transverse coordinate and z the longitudinal coordinate, corresponding to the direction of propagation of the tip. If V is the tip velocity, then we can consider the frame of reference advancing at this speed and introduce the new coordinate

$$\zeta=z-Vt\ . \tag{6}$$

In this frame of reference, we will consider that the diffusion field evolves in a quasisteady manner, so that the following equation is satisfied:

$$Lu=\Delta u+\frac{2}{l}\frac{\partial u}{\partial\zeta}=0\ , \tag{7}$$

where $l=2D/V$ is a diffusion length. Normally, Lu should be equal to the time derivative of u, but we can neglect this term in the quasisteady approximation. If we introduce the adjoint operator L^+ of L, and the Green's function $g(r,r')$ of the adjoint operator, defined as

$$L^+g(r,r')=-\delta(r-r')\ , \tag{8}$$

then this Green's function can be written as

$$g(r-r')=\frac{1}{2\pi}e^{(\zeta-\zeta')/l}K_0(|r-r'|/l)\ , \tag{9}$$

where K_0 is the modified Bessel function of zeroth order. It can be shown by use of Green's theorem [21] that the morphogen concentration u and its normal derivative on the interface can be related as

$$\int ds\, g(r,r')\frac{\partial u}{\partial n}(r)=\int ds\, h(r,r')u(r)\ , \tag{10}$$

where s is as before the curvilinear coordinate, the integration being taken on the whole interface, and h is the following function:

$$h(r,r')=\frac{1}{2\pi l}e^{(\zeta-\zeta')/l}\left[-n_z K_0(|r-r'|/l)-\frac{n(r-r')}{|r-r'|}K_l(|r-r'|/l)\right]-c(r')\delta(r-r') , \quad (11)$$

where K_1 is the modified Bessel function of the first order, n is the normal vector on the interface, and n_z the longitudinal component of the normal. It can also be shown that h satisfies the important formula

$$\int ds\, h(r,r')=-1 , \quad (12)$$

the integration being again taken on the whole interface.

At a given time step, the interface will be discretized as a finite number of points (x_j,ζ_j) where j varies from 1 to the number of points N. There is a unique circle which goes through three successive points of the mesh, thus defining the local normal vector and curvature. Between two points of the mesh, the interface is approximated by a straight line. Then we can calculate the functions $g(r,r')$ and $h(r,r')$ by formulas (9) and (11), the velocity V corresponding to the velocity of the tip at the previous time step, for any values r and r' of the interface, not only exactly on the mesh, but also in between. We calculate the morphogen concentration on the interface u_j by solving the integral equation (10). This equation can be discretized into a matrix equation linking the concentration on the mesh u_j and the normal derivatives of the concentration on the mesh:

$$\sum_{j=1}^{N} G_{ij}\left[\frac{\partial u}{\partial n}\right]_j=\sum_{j=1}^{N} H_{ij}u_j , \quad (13)$$

where the matrix coefficients G_{ij} and H_{ij} are integrals of g and h performed on segments between mesh points (see [21] for more details). These integrals are performed using standard Gauss quadrature methods, except in the cases where $j=i,i+1,i-1$, where the modified Bessel functions have a logarithmic divergence which must be taken into account with specific Gaussian integration formulas for integrands with a logarithmic singularity [22]. Furthermore, Eq. (12) makes it possible to calculate the diagonal coefficients H_{ii} by the formula

$$H_{ii}=-\sum_{j\neq i} H_{ij}-1 . \quad (14)$$

Thus we have to solve Eq. (13), the normal derivatives of the concentration on the interface being a function of the concentration through Eqs. (2) and (4). We solve this equation by an iterative process that converges toward the concentration on the mesh u_j.

Once the concentration has been calculated on the interface shape at a given time, we obtain the interface at the next time step by advancing each mesh point with the normal velocity given by Eqs. (3) and (5), the normal vector and curvature being calculated as explained above. Actually we suppose that the tip is symmetric and only calculate the positions of half of the interface points. Then we obtain the new value V of the tip velocity (we define it here as the normal velocity of the most advanced point of the interface); this new value of V defines a new diffusion length $l=2D/V$: it is thus possible to calculate the functions g and h corresponding to the new shape and diffusion length at the next time step.

The interface we solve numerically is not infinite and must be truncated at some point. However, the active zone of the tip is in practice not affected by the tail region if the integration domain is sufficiently extended, so this is a minor problem. Because of the propagation, the mesh points have a tendency to concentrate in some zones or to move apart in other regions, so that it is necessary to modify the mesh in the course of the calculation. Points are added where precision is not sufficient or suppressed where they are too close and could cause numerical instabilities.

IV. RESULTS

We will here obtain numerical solutions of the model described in the previous sections which have the form of an expanding tip, and show that these solutions are quite similar to experimental results. Furthermore, our calculations are limited to solutions growing in a quasistationary manner, and we will have to select initial conditions leading to such an evolution. Some initial solutions seem to lead to rapid transients that we cannot solve in the framework described in the previous section.

Apart from this condition of slow temporal evolution, the initial conditions will be relatively arbitrary, and we expect that a growing tip can emerge from this initial condition. After a sufficient period of growth, the tail will not influence the growth any more, so the initial conditions will not be important.

We first consider a case with high "effective rigidity." The normal velocity defined by Eq. (5) corresponds here to the parameters $a=33.33$, $b=2.66$, and $\gamma=10$. The time step in this calculation is limited to very low values because of numerical stability considerations. We show in Fig. 1 how the tip forms from the initial conditions. On this figure the initial solution and the solution at a later time are shown. At the initial time, there is a large zone of the interface which gets immediately frozen, i.e., it corresponds to a value of u below u^*, here -0.08 [see Eq. (5)]: the two solutions are practically superposed in this zone because the frozen region extends when the tip advances. From this initial solution, an advancing

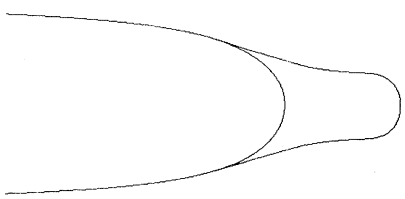

FIG. 1. Cell shape for two different times at the beginning of growth (parameters $a=33.33$, $b=2.66$, and $\gamma=10$): the lower curve corresponds to the initial condition; in the upper curve a rhizoid is beginning to form.

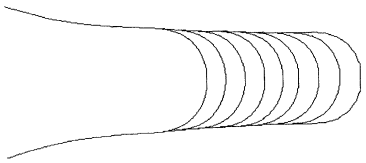

FIG. 2. Continuation of the evolution of Fig. 1: cell shape for nine different times showing the propagation of a stationary rhizoid.

rhizoid begins to form, as seen on the upper curve of Fig. 1, and this rhizoid becomes narrower as time increases.

Then the tail region becomes completely unimportant, and it is possible to cut the far tail, which is only a residue of the initial conditions, without changing anything in the rhizoid growth. We have proceeded in this manner, and the result of the subsequent evolution of the rhizoid is shown in Fig. 2, where several shapes corresponding to different times are plotted. It can be seen that after the transient just described the tip grows with a nearly constant shape and velocity. This propagating stationary solution of the equations closely resembles the growing rhizoid observed in various biological systems, such as the neuron axon or the fungal hyphal cells [19]. Solutions of this type were also produced by the geometrical model of [7] in the case of high rigidity. In our simulation, sufficiently far away from the tip the growth is simply frozen; the region of the active zone close to the frozen zone is completely dominated by the rigidity term: the shape must be close to a straight line because otherwise the normal velocity would be extremely great. At a later time this zone will also become frozen, and this explains the rhizoid shape we obtain. It is important to note that for any functions $v(u)$ and $j(u)$ increasing the effective rigidity always favors the growth of rhizoids, even though high values of this parameter seem necessary to obtain a pure cylindrical shape.

In Fig. 3, we show the morphogen concentration on the interface versus the curvilinear coordinate, for the shape corresponding to the first plot of Fig. 2. This figure is symmetric relative to the maximum of concentration located at the tip. Moving away from the tip, the concentration decreases a lot, except in the far tail region, where it increases a little. This region corresponds to the zone where the stationary rhizoid is not completely formed. If we examine the effects of this concentration on the morphogen influx, then the concentration maximum corresponds to a maximum influx, but it is important to note that, u being greater than u_0 on the whole domain [see Eq. (4)], the morphogen flux enters the cell in the whole interface. Concerning the concentration effects on the normal velocity [see Eq. (5)], the velocity caused by concentration (there is also a part of the velocity caused by curvature effects) is maximum at the tip and then decreases quickly. Finally a large part of the tail has a concentration below u^* and is frozen.

We consider now a typical case corresponding to an advantage tip at low rigidity: the normal velocity defined by Eq. (5) corresponds to the parameters $a=66.66$, $b=5.66$, and $\gamma=0.1$ [the slope of the function $v(u)$ is here higher than in the previous case, and this will cause the tip to enlarge during the growth]. We show in Fig. 4, as before, the shapes of the front at different times (the different shapes are not plotted at equal time intervals). The lower curve corresponds to the initial conditions. It represents a relatively flat sort of tip, which is observed experimentally at the beginning of tip formation in the desmid (a sort of unicellular alga) *Micrasterias rotata* [3]. Although almost flat, the tip is actually slightly curved towards the cell interior. In the second plot on the same figure, the tip has advanced and has been enlarged. This effect has been called lobe broadening in the experiments [3]. Furthermore, the curvature has begun to change sign, although this is a very small effect and cannot be seen yet on the plot. In the third plot of the same figure, it is now possible to see that the tip is curved towards the cell exterior. This effect is amplified in the fourth plot,

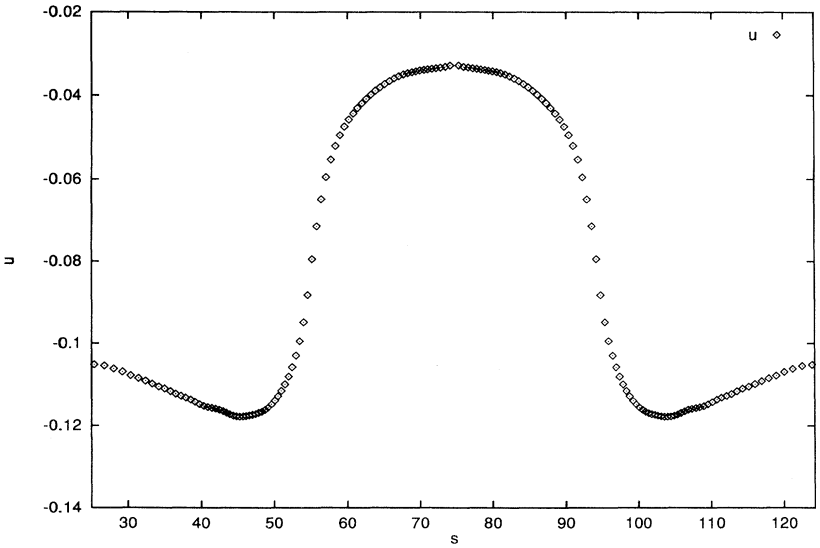

FIG. 3. Morphogen concentration versus curvilinear coordinate on the membrane for the first solution of Fig. 2: there is a maximum of concentration at the tip.

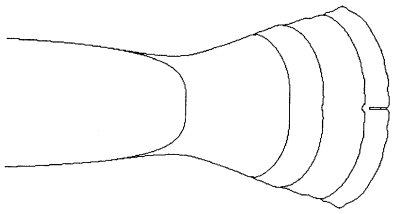

FIG. 4. Cell shape for five different times (parameters $a=66.66$, $b=5.66$, and $\gamma=0.1$). The lower curve corresponds to the initial conditions. The formation of a stiff hollow zone at the tip can be observed.

where the hollow in the tip becomes more localized. Finally, in the fifth plot, the hollow becomes suddenly much deeper and thinner. It can be observed that the morphogen concentration has very rapidly dropped because of screening effects and that at the moment where the plot is taken the concentration in the hollow is so low that the growth is completely frozen in this zone. This explains why the hollow is becoming deeper so quickly.

In Fig. 5, an enlargement of the three last plots of Fig. 4 is shown. The first plot corresponds to a low curvature at the tip, and no other perturbations can be seen. On the second plot, the curvature at the tip has been amplified and at the same time perturbations around this hollow region are now visible. Finally, in the last plot, the hollow has become much stiffer. It has been quite difficult to obtain this solution numerically because it is practically mandatory to adapt the mesh in the course of the calculation to prevent too many mesh points from concentrating in the hollow zone, thus leaving other regions with a very low precision.

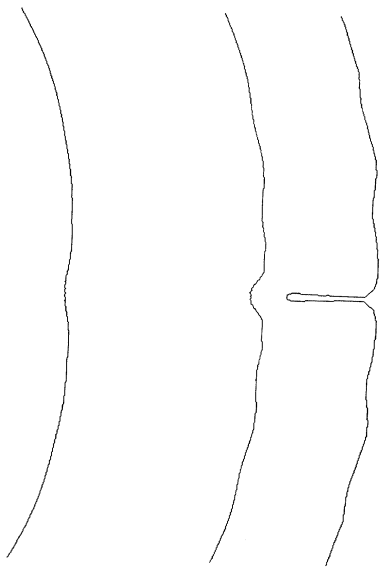

FIG. 5. Enlargement of the three last curves of Fig. 4.

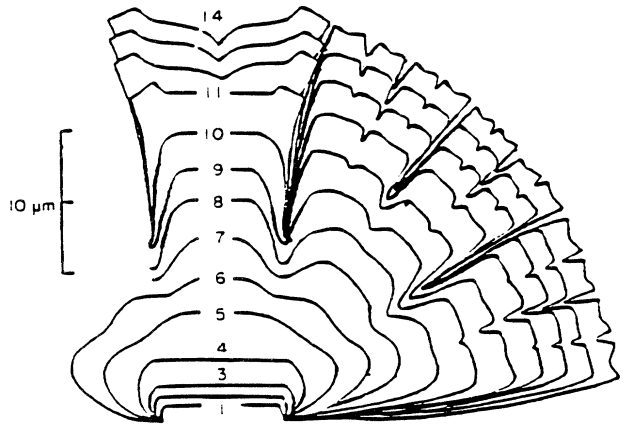

FIG. 6. Experimental cell shape for different times of a semicell of the alga *Micrasterias rotata* (courtesy of T. C. Lacalli: reprinted from [3] with the permission of the Company of Biologists Ltd.).

It may seem that this hollow formation is a strange effect; however, it has been observed in *Micrasterias rotata* [3] and is called lobe branching. In Fig. 6, a picture taken from [3] is shown: on this figure it is possible to see on different lobes the two effects of lobe broadening and of lobe branching obtained in the simulation. This last effect was also seen in the geometrical model [7], and is of course related to the tip splitting observed, for instance, in crystal growth [21]. However, in our simulations and in the experiments, the hollow zone is much stiffer than the lobe branching produced in the geometrical model. We have not continued our simulation after the last plot of Figs. 4 and 5, but in the experiments the new lobes produced after the lobe branching break in two again some time later (see Fig. 6).

V. CONCLUSION

A model for cellular tip growth has been simulated numerically. In this model, growth is coupled to a diffusive morphogen located outside the cell. The influx of morphogen at the membrane and the normal velocity of the interface are supposed to be functions of the concentration. It has been possible to solve the equations of this model in a quasistationary approximation by using a Green's function formalism previously developed in crystal growth. Simulations have shown that two typical effects encountered in tip growth are contained in this model: the pure rhizoid growth leading to cylindrical tubes observed in a variety of cells, such as fungal hyphae or neurons, but also lobe broadening and a sort of tip splitting called lobe branching, which are observed in unicellular algae. It seems that in order to obtain rhizoids an important effective rigidity of the interface is necessary.

ACKNOWLEDGMENTS

Fruitful discussions with P. Pelcé and M. Leonetti are gratefully acknowledged.

[1] *Plant Physiology,* edited by L. Taiz and E. Zeiger (Benjamin Cummings, Redwood City, CA, 1991).
[2] *Tip Growth in Plant and Fungal Cells,* edited by I. P. Heath (Academic, San Diego, 1990).
[3] T. C. Lacalli, J. Embryol. Exp. Morphol. **33**, 95 (1975).
[4] P. Pelcé, *Dynamics of Curved Fronts* (Academic, San Diego, 1988).
[5] Pierre Pelcé and A. Pocheau, J. Theor. Biol. **156**, 197 (1992).
[6] R. C. Brower *et al.*, Phys. Rev. Lett. **51**, 309 (1983).
[7] Pierre Pelcé and J. Sun, J. Theor. Biol. **160**, 375 (1993).
[8] H. G. E. Hentschel and A. Fine, Phys. Rev. Lett. **73**, 3592 (1994).
[9] Lionel G. Harrison and M. Kolar, J. Theor. Biol. **130**, 493 (1988).
[10] F. M. Harold and J. H. Caldwell, in *Tip Growth in Plant and Fungal Cells* [2].
[11] D. L. Kropf, Microbiol. Rev. **56**, 316 (1992).
[12] P. Pelcé, Phys. Rev. Lett. **71**, 1107 (1993).
[13] B. Denet and P. Pelcé, Europhys. Lett. **25**, 265 (1994).
[14] R. Larter and P. Ortoleva, J. Theor. Biol. **96**, 175 (1982).
[15] F. M. Harold, Biosci. Rep. **11**, 347 (1991).
[16] W. J. A. Schreurs, R. L. Harold, and F. M. Harold, J. Gen. Microbiol. **135**, 2519 (1989).
[17] J. Q. Zheng *et al.*, Nature **368**, 140 (1994).
[18] C. W. Cho, F. M. Harold, and W. J. A. Schreurs, Exp. Mycol. **15**, 34 (1991).
[19] J. H. Burnett and A. P. J. Trinci, *Fungal Walls and Hyphal Growth* (Cambridge University Press, Cambridge, England, 1979).
[20] D. I. Meiron, Phys. Rev. A **33**, 2704 (1986).
[21] Y. Saito, G. Goldbeck-Wood, and H. Muller-Krümbhaar, Phys. Rev. A **38**, 2148 (1988).
[22] *Handbook of Mathematical Functions,* edited by M. Abramowitz and I. A. Stegun (Dover, New York, 1972).